



INVESTIGATIONS ON THE GROWTH AND CHARACTERIZATION STUDIES OF NONLINEAR OPTICAL SINGLE CRYSTAL L-PROLINE ZINC ACETATE

T GURUMURTHI^{1*}, MESFIN ASFAW AFRASSA¹, ANNO KARE ANNO¹ and P MURUGAKOOTHAN²

¹School of Applied Natural Sciences (Physics), Adama Science and Technology University, Ethiopia.

²MRDL, PG and Research Department of Physics, Pachaiyappa's College, Chennai, India.

Abstract

A nonlinear optical material L-Proline Zinc acetate was synthesized and grown as single crystals by slow evaporation method. The grown crystals were subjected to structural, elemental, thermal, optical and dielectric studies. The structural analysis reveals that L-Proline Zinc acetate belongs to the monoclinic crystallographic system with space group P_{21} . Optical transparency of the grown crystals was investigated by UV-vis-NIR spectrum. The thermal analyses reveal that L-Proline Zinc acetate is thermally stable up to 163°C . The dielectric constant and dielectric loss of the crystals were studied as a function of frequency. The nonlinear optical property of the doped crystal was confirmed by the Kurtz-powder second harmonic generation test.

Keywords: Growth from solution, Nonlinear optical crystal, X-ray diffraction, Semi organic compound, Thermal and Dielectric.

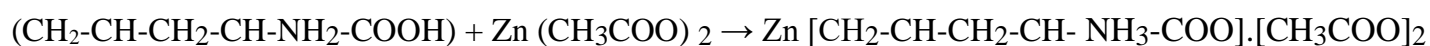
1. Introduction

The growth of nonlinear optical (NLO) crystal has become a focus of current research in view of their potential applications in various photonic technologies such as optical communication, optical data storage and information processing, etc..[1-5]. Currently the need is to find and to grow new NLO crystals which are transparent in the visible region and possessing enhanced hyperpolarizabilities and satisfying at the same time all the technological requirements for applications[6-8]. Research in the development of NLO crystals, is being carried out under three different areas such as: Discovery of new efficient NLO materials, Bulk growth of promising NLO crystals to explore the various optical behaviour and Improving the characteristics of NLO crystal by suitable doping. Motivated by the above considerations and based on the literature survey, this paper has been formulated with the following objectives: To synthesize the material and to grow L-Proline Zinc acetate (**LPZA**) ($Zn(C_5H_9NO_2).(CH_3COO)_2$), to characterize the grown crystals in order to understand its structural, vibrational, elemental, optical, thermal, electrical and mechanical properties based on the following studies: X-ray diffraction analysis (by the single crystal and by the powder method), FTIR spectral analysis, Elemental analysis, UV spectral studies, Thermal analysis (TGA/DTA/DSC), Dielectric studies, Microhardness studies and Nonlinear measurements (SHG).

2. Experimental

1. Materials and Methods

The starting materials L-Proline ($C_5H_9NO_2$) and zinc acetate ($Zn(CH_3COO)_2$) (analytical grade reagents) were taken in the equimolar ratio. The calculated amount of L-Proline was first dissolved in double distilled water. Then zinc acetate was slowly added to the solution with continuous stirring using magnetic stirrer. The prepared homogeneous mixture of solution was let to dry at room temperature. LPZA salt was synthesized according to the reaction:



The purity of the synthesized salt was improved by the successive recrystallization process. Care was taken during heating of the solution and a maximum temperature of 50°C was maintained in order to avoid decomposition. The melting point of LPZA salt was observed to be 216.2°C.

2. Solubility diagram

The solubility test gives us idea to select the suitable solvent and temperature to grow good quality single crystals. The solubility of a material in a solvent decides the amount of the material which is available for growth and hence determines the size of the crystal that can be grown [9]. This solubility procedure was repeated for water, ethanol and methanol in the range 30-50°C. The solubility curve was drawn between temperature and concentration. The solubility curve of LPZA is shown in Fig. 1. It is

found that the sample exhibits a positive temperature gradient and water is found to be the best solvent to grow the single crystals by slow evaporation technique.

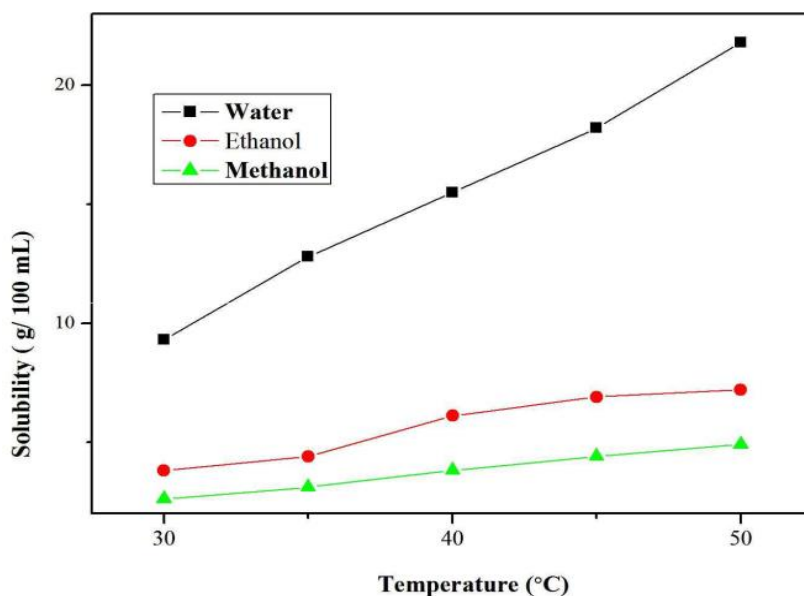


Fig. 1: Solubility curve of LPZA

3. Crystal growth of LPZA

Saturated solution was prepared (pH = 5.08) using recrystallized salt of LPZA with double distilled water as solvent at 35°C temperature. The prepared solution was filtered using Whatmann 41 filter paper to remove the suspended impurities. The solution was taken in beaker and covered with perforated paper. The covered beaker with saturated solution was kept in CTB at 35°C with accuracy of $\pm 0.01^\circ\text{C}$. LPZA single crystal of size $24 \times 26 \times 16 \text{ mm}^3$ was grown by slow evaporation technique and harvested in a growth period of 25 days and is shown in Fig. 2.



Fig. 2: Photograph of as grown crystal of LPZA

4. Characterization

The Grown single crystal LPZA was subjected to X-ray diffraction studies using a Bruker AXS Kappa APEX II single crystal CCD diffractometer equipped with graphite monochromated Mo(K α) ($\lambda = 0.7107 \text{ \AA}$). The CHNS analysis for all the grown crystal was carried out using an instrument Elementar Vario EL III-GERMANY, CHNS analyzer. HIOKI 3532 – 50 LCR HITESTER was used for the dielectric study. The sample of size $3 \times 3 \times 2 \text{ mm}^3$ was prepared and mounted between copper electrodes. In order to ensure good electrical contact between the crystal and the electrodes, the crystal faces were coated with silver paint. The dielectric measurements were carried out in a frequency range 100 Hz – 5 MHz and temperature range 35 – 95 °C.

The Thermo gravimetric and Differential thermal analyses (TG, DTA & DSC) response curves was drawn for LPZA powder sample in the temperature range from 20 to 1400 °C using the instrument NETZSCH STA 409C at the heating rate of 10 K/min. in nitrogen atmosphere. The optical transmission spectra were recorded using Shimadzu model - 1601 in the wavelength range of 300 – 1200 nm. The study of NLO conversion efficiency was carried out by the powder technique of Kurtz and Perry. The sample was ground into fine powder and tightly packed in a micro capillary tube. It was mounted in the path of the laser beam. A Q-switched flash lamp pumped Nd:YAG laser of power 3.2 mJ with a wavelength of 1064 nm, pulse duration of 8 ns, a repetition rate of 10 Hz and a spot size of 1 mm diameter was used for SHG test. Vickers hardness study was made on the as grown crystal using Leica-Reichert Polyvar2 model hardness tester fitted with a diamond indenter.

3. Results and discussion

1. Single crystal XRD analysis of LPZA

Lattice parameters of LPZA crystal were obtained by single crystal XRD analysis and shown in Table 1. These parameters are compared with L-Proline [10]. From this study it was found that the LPZA crystallizes in monoclinic system ($\beta = 112.73^\circ$). The volume of the cell is 792 \AA^3 .

Table 1: Lattice parameters of LPZA

Samples	a (Å)	b (Å)	c (Å)	β (°)	Unit Cell Volume (Å) ³	Crystal System
LPZA	10.02	6.43	13.33	112.73	792	Monoclinic
L-Proline	9.701	5.261	11.953	90.66	610	Monoclinic

9. Powder XRD analysis of the grown crystals

X-ray diffraction pattern was recorded by crushing the grown crystal into fine powder and the powder sample was scanned over the 2θ range $10-80^\circ$ at a rate of 1° per minute. All the reflection planes are identified and the obtained 2θ values are used for indexing using Check cell software package. The indexed powder X-ray diffraction pattern of the LPZA crystal is shown in Fig. 3. The well defined and sharp peaks imply the good crystalline nature of the compounds.

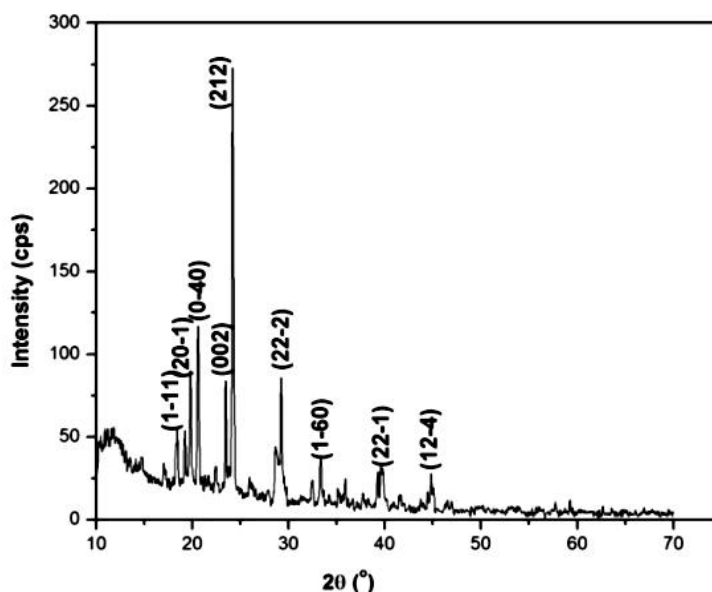


Fig. 3: Powder XRD spectrum of LPZA

10. FTIR spectral studies of LPZA

The recorded FTIR spectrum of LPZA is shown in Fig. 4. Considering the molecular structure of L-Proline, the vibrations of crystalline L-Proline zinc acetate may be arisen due to internal vibration of functional groups NH_3^+ , CH, CH_3 and COO^- . The presence of broad band in high wave number region indicates the presence of hydrogen bonds [11]. A broad strong absorption in the region $3400 - 2100 \text{ cm}^{-1}$ corresponds to the NH_3^+ ion of the amino acid. Generally N-H and O-H bonds participate in hydrogen bonding. In LPZA crystal, the valine molecule is protonated at amino group (NH_3^+) and deprotonated at the carboxylate group (COO^-). The protonation of amino group can be proved because of the presence of strong band at 1611 cm^{-1} (asymmetric deformation of NH_3^+). The asymmetric stretching vibration of NH_3^+ ion for L-Proline appeared at 3089 cm^{-1} . This band is shifted in LPZA at 3060 cm^{-1} . Moreover, the presence of absorption bands at $2632, 2431, 2213, 2019$ and 1896 cm^{-1} can be attributed to the overtone and combination bands of NH_3^+ bending and C-H stretching vibration overlapping. The presence of COOH is indicated by a sharp absorption band at 1706 cm^{-1} , which is due to the C=O stretching mode of COOH group [12].

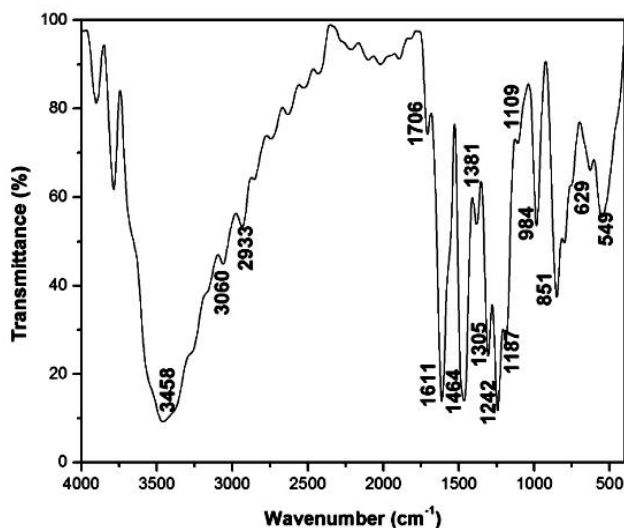


Fig. 4 : FTIR spectrum of LPZA crystal

11. Elemental Analysis

Before starting the experiment, the instrument was calibrated carefully and the measurements has a precision of 0.05% by weight. The experimental values obtained are compared with the calculated values and presented in Table 2. The experimental value of the grown crystal is in good agreement with the calculated values. Thus elemental analysis fairly confirms the formation of the new crystal compounds.

Table 2: Elemental analysis of the grown crystals

Sample	Weight (mg)	Carbon (%)		Hydrogen(%)		Nitrogen (%)	
		Expt.	Cal.	Expt.	Cal.	Expt.	Cal.
LPZA	8.6243	40.89	41.17	4.01	4.22	5.08	5.33

12. Thermal analysis of LPZA

The recorded TGA/DTA spectra of the LPZA sample are shown in Fig. 4.1. Heating was carried out at a rate of 20°C /min. The initial mass of the material subjected to analysis was 2.9970 mg and the final was only 0.3630% of the initial mass at temperature of about 1100°C indicating bulk decomposition occurring into LPZA crystals. From the TGA curve, the thermal stability of the sample is realized up to 163°C and there after the material shows loss in weight due to the molecules, which are loosely bounded to the metal ion. The major 70% of weight loss between 208°C to 279°C is due to the liberation of volatile substances.

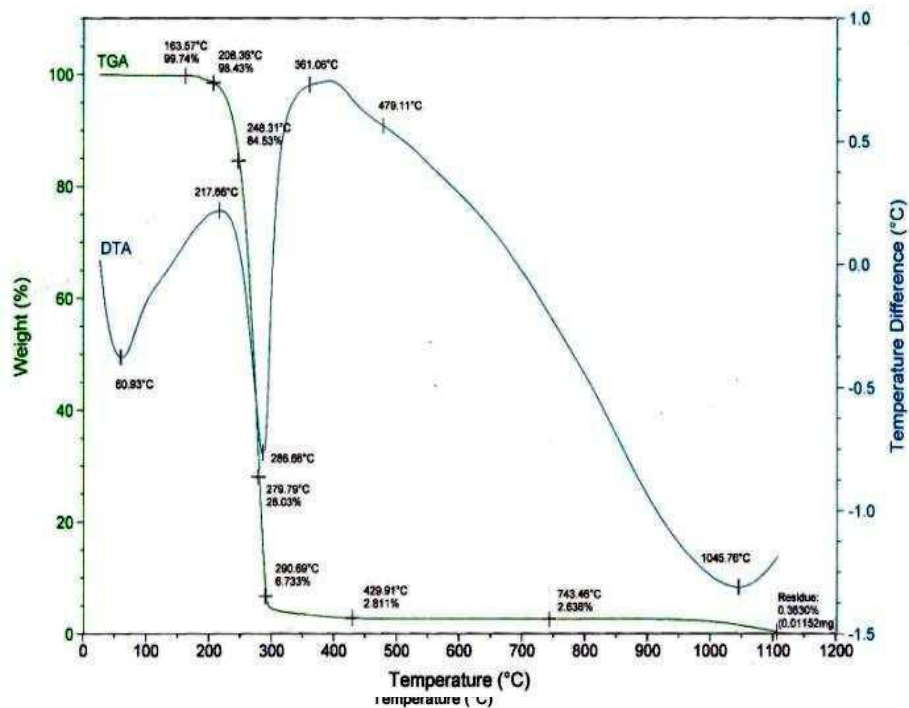


Fig. 5: TGA/DTA curves of LPZA

It is observed from DTA curve, that the material undergoes exothermic transition at about 217°C where the decomposition starts. The material is fully decomposed at an irreversible endothermic transition at about 286°C. It is inferred that the melting point of the material takes place in the vicinity of 217°C. The sharpness of the endothermic peak shows good degree of crystallinity of the grown LPZA. The observed DSC spectrum of the LPZA crystal is shown in Fig. 4.2. From DSC spectrum, the specific heat capacity of the LPZA crystal is 649 J/g°C observed at 286°C.

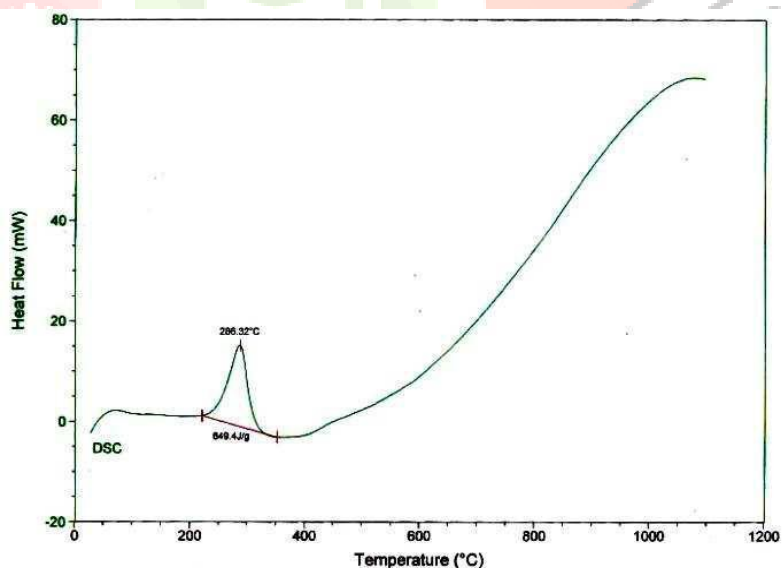


Fig. 6: DSC curve of LPZA

13. Vickers hardness measurement

Micro indentation is made on the surface of a specimen with the help of a diamond indenter. The Vickers pyramid indenter where opposite faces contain an angle ($\alpha = 136^\circ$) is most widely accepted pyramid indenter. Indentations were carried out at different loads in the range 25 - 100 g. The Vickers hardness (H_V) was calculated from the relation [13],

$$H_V = \frac{1.854P}{d^2} \text{ kg/mm}^2$$

The hardness values increase with the increase of the applied load. Usually a decrease in apparent micro hardness with increasing applied load which may be arised due to work hardening, initiate plastic deformation, size of dislocation loops etc,. At small loads, the indenter penetrates only the surface layers and therefore, the effect is shown sharply at the early stages. When the applied load increases, the penetration depth also increases and the overall effect must be due to the surface and inner layers. Consequently in this stage, indentation depth increases proportionally with applied pressure.

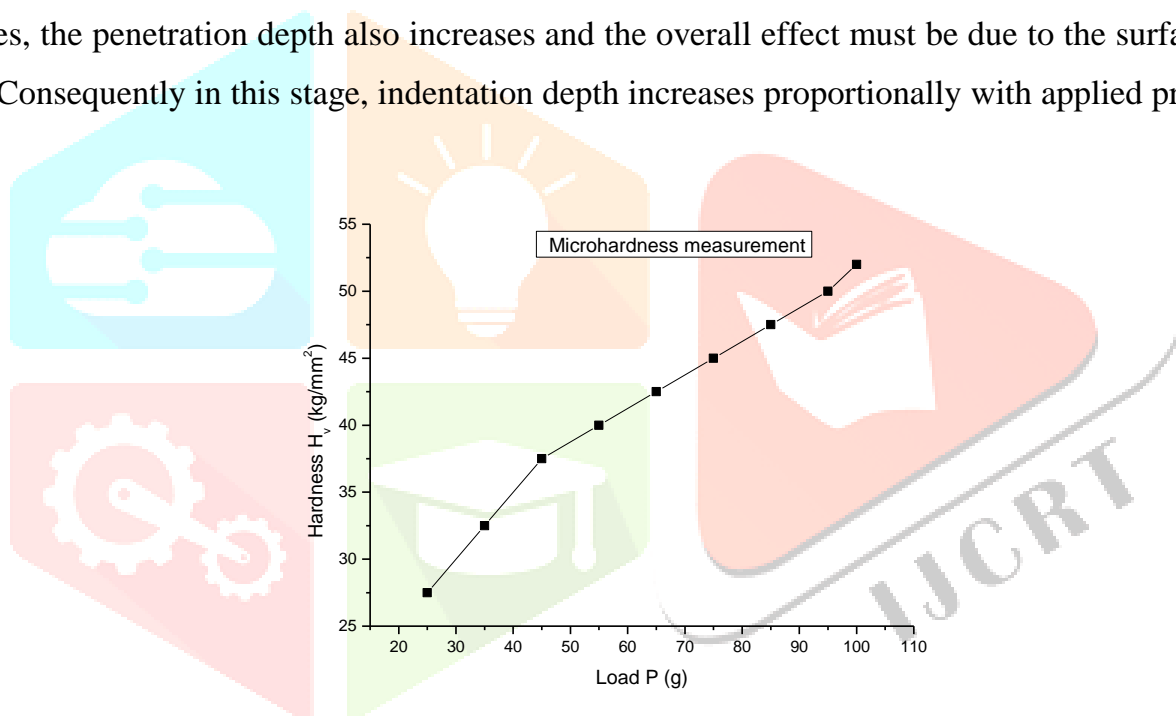


Fig. 7: Variation of Vickers constant as a function of load

14. Dielectric studies of the grown crystal

A graph was drawn between the calculated values of dielectric constant (ϵ') and log frequency. Fig. 8 shows the variation of dielectric values with various frequencies for the grown crystal LPZA at different temperatures. The dielectric constant decreases with increase in frequency for all temperatures and this is termed as anomalous dielectric dispersion [14]. This is a normal dielectric behaviour and can be understood on the basis of internal polarization process [15]. The dielectric constant value depends on the degree of polarization charge displacement in crystal. The dielectric constant of material is due to the contribution of electronic, ionic, dipolar and space-charge polarizations which depend on the frequencies. All these polarizations are active at low frequencies (below 10 KHz). The space charge polarization is generally active at lower frequencies and at higher temperatures [16].

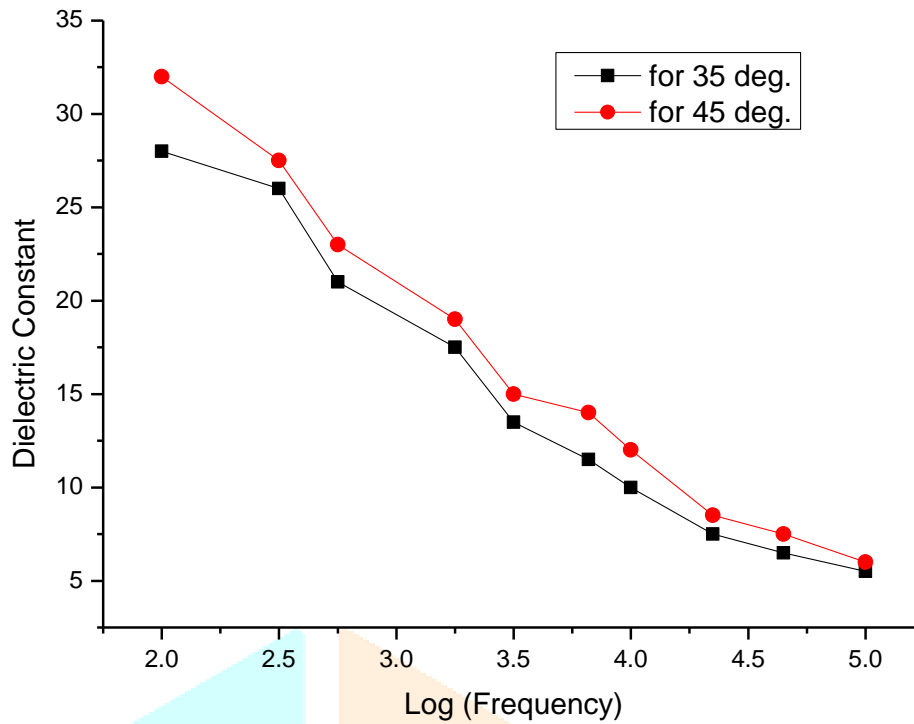


Fig. 8: Dielectric constant of LPZA as a function of frequency at 35°C & 45°C

A material must have low dissipation factor for device fabrication. Dielectric loss values were calculated from the experimental observations and the graph is drawn between the dielectric loss and frequency values. Fig. 9 shows the variation of dielectric loss with applied frequency of the field for the grown crystal LPZA. Fig. show the low dielectric loss at high frequencies suggests that the samples have lesser defects. Also at lower frequencies and at high temperatures, the dissipation factor is due to space charge polarization owing to charged lattice defects [17]. The charge carriers can migrate some distance under the influence of applied fields. Due to blocking of charge carriers at the cathode, space charge region is developed and there will be substantial increase of dielectric loss at lower frequencies. Also the hopping of charge carriers on the lattice surface is thermally activated by an increase in the temperature. Thus the gradual decrease of loss at higher frequency clearly shows defect free optical quality crystals.

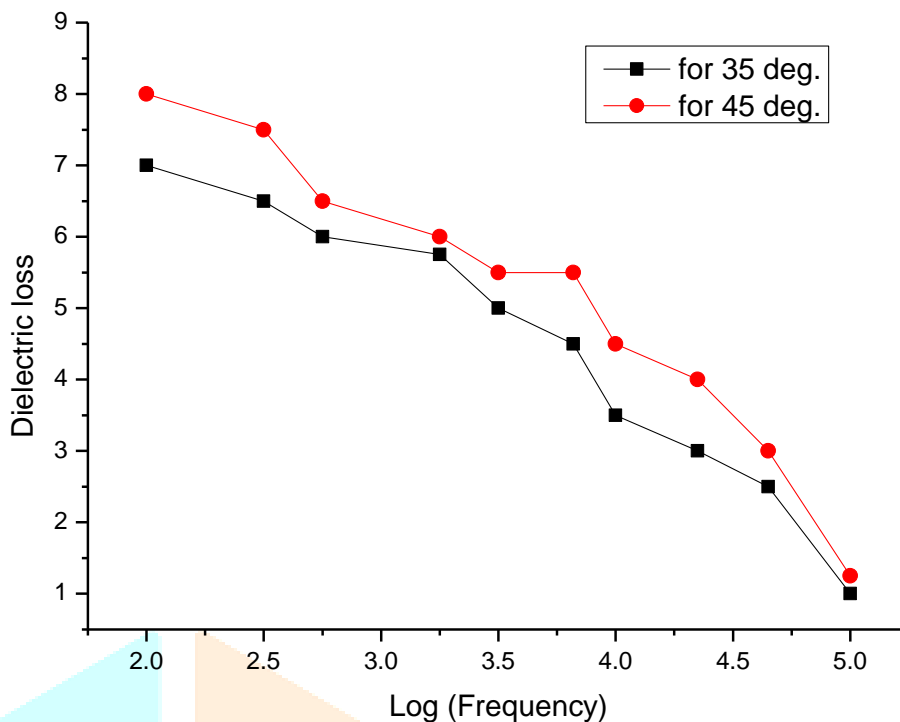


Fig. 9: Dielectric loss of LPZA as a function of frequency at 35°C & 45°C

15. Optical transmission study

The fig. 10 shows the optical transmission spectra of LPZA crystal. The thickness of the sample used for this study was 2 mm. It is found that LPZA crystal has transmittance of 66 %. The lower cut off for LVP is 470 nm. Semi organic complex LPZA show their wide transparency in the visible region due to amino acid combination with inorganic metal salts.

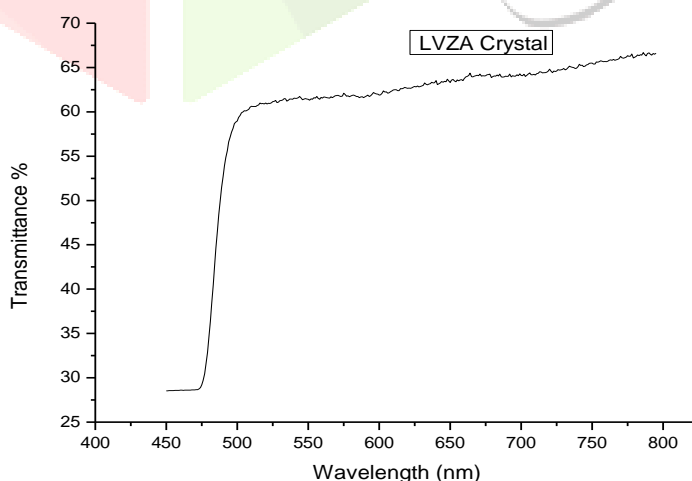


Fig. 10: Optical transmission for LPZA crystal

16. *SHG efficiency of the grown crystal*

In the present work, the SHG efficiency of the powdered samples LPZA was found relatively with KDP. The measured values are presented in Table 3. In semi organic crystals, delocalization of electrons are promoted due to metal ions. Hence LPZA have good relative SHG efficiencies than other organic crystals. Since the second order non linear efficiency will vary with the particle size of powder sample [18], the care has been taken to maintain uniform particle size of source and the reference material.

Table 3: Relative SHG efficiency of the grown crystals

Sample	Laser power (mJ/p)	SHG efficiency of sample (mV)	SHG efficiency of KDP (mV)	Relative SHG efficiency
LPZA	2.4	48	35	1.37

4. **Conclusions**

Metal organic LPZA material was synthesized, purified and used for solubility studies to find the suitable solvent and temperature to grow good quality single crystals. Good optical quality bulk single crystals were grown with synthesized recrystallized salts from aqueous solution by slow evaporation technique. The structural characterization of the grown crystals was done by single crystal and powder X-ray diffraction studies. From these studies it was found that the LPZA was crystallized in monoclinic system. The indexed powder X-ray diffraction pattern of the grown crystal show the well defined sharp peaks which imply the good crystalline nature of the compound. FTIR spectral studies of the grown crystal confirmed the presence of functional groups in the compound. Elemental analysis gave the details of percentage of element present in the newly formed crystal sample. The experimental value obtained was in good agreement with the calculated values and the analysis confirmed the formation of the new crystal compound.

Thermal analysis of the grown crystals showed the thermal stability of the compounds. TGA of LPZA showed 70% weight loss between 208-279°C and the specific heat capacity was found to be 649 J/g/°C at 286°C. Microhardness of the crystal was performed by Vickers micro hardness test and the hardness increases with the increase of load. From the dielectric measurements, dielectric parameters such as dielectric constant and dielectric loss were calculated. The variation of dielectric constant in metal complex LPZA revealed that, the inclusion of metal ion into amino acid decreases the dielectric constant value. Low dielectric loss at higher frequencies suggests that the sample crystals have lesser defects. UV-vis-NIR spectral study was employed to understand the linear optical properties of the grown crystals. The SHG efficiency of the powdered samples of all the grown crystals was found relatively with KDP by modified Kurtz- Perry technique. LPZA have good relative SHG efficiency.

References

- [1]. Bloembergen, N., *Nonlinear Optics*, fourth ed., World Scientific, Singapore, New Jersey, London, Hong Kong, 1996.
- [2]. Franken, P.A., Hill, A.E., Peters, C.W., Weinreich, G., Generation of optical harmonics, *Phys. Rev. Lett.*, 7 (1961) 118-119.
- [3]. Williams, D. J., Large optical nonlinearities, *Angew. Chem. Int. Ed. Engl.*, 23 (1984) 690-703.
- [4]. Boyd, R.W., *Nonlinear Optics*: Academic press, New York, 1992.
- [5]. Franken, P.A., Ward, J.F., Optical Harmonics and nonlinear phenomena, *Rev. Mol. Phys.* 35 (1963) 23-39.
- [6]. Shen, Y.R., *The Principles of Nonlinear Optics*: Wiley, New York, 1984.
- [7]. Bergman, J. G., Boyd, A., Ashkin, S., Kurtz, K., New nonlinear optical materials: Metal oxides with nonbonded electrons, *J. Appl. Phys.*, 40 (1969) 2860- 2862.
- [8]. Prasad, P. N. Reinhardt, B. A., Is there a role for organic materials chemistry? *Chem. Mater.*, 2 (1990) 660-669.
- [9]. Ushasree, P.M., Muralidharan, R., Jayavel, R., Ramasamy, P., Metastable zone width, induction period and interfacial energy of Zinc tris (thiourea) sulfate, *J. Cryst. Growth*, 210 (2000) 741-745.
- [10]. Moitra, S., Kar, T., Growth and characterization of L-Valine - nonlinear optical crystal, *Cryst. Res. Technol.*, 45 (2010) 70-74.
- [11]. Dalhus, B., Gorbitz, C.H., Crystal structures of hydrophobic amino acids¹. Redeterminations of L-Methionine and L-Valine at 120 K, *Acta. Chem. Scand.*, 50 (1996) 544-548.
- [12]. John Coates, Interpretation of Infrared spectra, A Practical Approach in *Encyclopedia of Analytical Chemistry*, Meyers, R.A., (Ed.) (John Wiley & Sons Ltd., Chichester (2000) pp.10815-10837.
- [13]. Mott, B.W., *Micro Indentation Hardness Testing*, Butterworth, London, 1956.
- [14]. Wang, X.Q., et al., Crystal growth and physical properties of UV nonlinear optical crystal Zinc Cadmium thiocyanate $ZnCd(SCN)_4$, *Chem. Phys. Lett.*, 346 (2001) 393-406.
- [15]. Senthil Murugan, G., Ramasamy, P., Growth and characterization of metal organic crystal: Tetra thiourea Cobalt chloride, *J. Cryst. Growth* 311 (2009) 585-588.
- [16]. Prasad, N.V., Prasad, G., Bhimasankaran, T., Suryanarayana, S.V., Kumar, G.S., Studies in $(NH_4)_2xCd_{1-x}C_2O_4 \cdot H_2O$ single crystals grown by gel technique, *Ind. J. Pure. Appl. Phys.*, 34 (1996) 834-836.
- [17]. S.K. Arora, Vipul Patel, Brijesh Amin, Anjana Kothari, Dielectric behaviour of Strontium tartrate single crystals, *Bull Mater. Sci.*, 27 (2004) 141-148.
- [18]. Bergman, J. G., Boyd, A., Ashkin, S., Kurtz, K., New nonlinear optical materials: Metal oxides with nonbonded electrons, *J. Appl. Phys.*, 40 (1969) 2860- 2862.